RSC Advances

PAPER

View Article Online
View Journal | View Issue

Cite this: *RSC Adv.*, 2023, **13**, 17282

Synthesis, structural studies and computational evaluation of cyclophanes incorporating imidazole-2-selones†

Ahmed Hassoon Mageed * and Karrar Al-Ameed

We report new cyclophanes containing imidazole-2-selone groups linked by xylylene rings. A set of imidazole-2-selone cyclophanes is synthesized by reaction corresponding to imidazolium cyclophanes with selenium in the presence of K_2CO_3. The structural behavior of the new imidazole-2-selone cyclophanes was determined by ^1H and ^{13}C NMR spectra and X-ray diffraction studies. Cyclophanes incorporating *o*-xylylene or mesitylene-*m*-cyclophane linked by selone groups were mutually *syn* in both the solid state and solution, and the cyclophanes showed a conformation similar to the cone conformation of calix[4]arenes. Cyclophanes incorporating *p*-xylylene or *m*-xylylene linked by selone groups showed two conformations in the solution: one mutually *syn* and the other mutually *anti*. There was no interconversion for both conformations observed on the NMR timescale. In the solid state, three conformations were detected for the *p*-xylylene-linked cyclophane: one is mutually *syn* and the other two are mutually *anti* and partial cone conformations. In the *m*-xylylene-linked case, only *anti*-conformation was characterized in the solid state. A density functional analysis was conducted to interpret the stability of the studied compounds and shed light on their origin. The energy preference analysis is in consistent agreement with the observed geometries and their co-existence.

Received 2nd May 2023
Accepted 17th May 2023

DOI: 10.1039/d3ra02913a

rsc.li/rsc-advances

Introduction

N-Heterocyclic carbenes (NHCs) can be used in various fields for different purposes, including organo transition-metal chemistry, catalysis, and the fields of biochemistry and medicine.[1–7] Interestingly, NHCs can act as σ-donor and π-acceptor ligands, which made them interesting chemical structures in different fields of chemistry.[1,8,9] Recently, NMR studies have been reported to determine the π-acceptor strength of NHCs by measuring the ^{31}P or ^{77}Se NMR chemical shifts of NHC–phosphinidene or NHC–Se adducts.[10–13] In particular, X-ray studies of NHC–S adducts showed that the NHC–S moiety is planar and that the C–S bond distance (~1.70 Å) is longer than a typical C=S bond distance (~1.63 Å).[14–19] Phosphinidene, selenium and sulfur adducts can be represented as the resonance hybrid by two structures (Fig. 1): the neutral hetero-alkene (**A**) with C=P/Se/S character and a zwitterionic structure (**B**) with a C–P/Se/S character.[12,14,15,20,21]

Recently, NHC selenium adducts (selones) have received significant attention owing to their promising applications, such as catalysis and their relevance in medicinal chemistry.[22–32] The first NHC-based selone was synthesized by reacting *o*-phenylenediamine with carbon diselenide in CCl_4 to form 2-isoselenocyanatoaniline **1**, and then product **1** was cyclized by the intermolecular reaction of isoselenocyanate with an amino group to obtain selone **2** in high yield (Scheme 1A).[33] The interesting procedure of synthesis of stable selone compounds is by the reaction of an imidazolium salt with base and then the addition of elemental selenium. For example, diarylimidazolium salt reacts with selenium to form 1,3-diarylimidazole-2-selenones **3** (Scheme 1B).[34]

Previously, we reported the synthesis of some cyclophanes, including imidazole-2-thione units, such as **4–7**, from corresponding imidazolium-linked cyclophanes (Fig. 2), and we studied their interesting conformational behaviour using X-ray diffraction and NMR studies.[18] Many imidazole-2-selones are known.[12,32,34–42] However, there are no reports of cyclophanes incorporating imidazole-2-selone moieties. As an extension of our study with imidazole-2-thiones, herein, we report the first synthesis of some cyclophanes, including imidazole-2-selone moieties, and study their conformational behaviour in solution and the solid state as well as use DFT calculations. Imidazole-2-selone cyclophanes may have great potential in various fields, including medicinal chemistry, catalysis, materials science, and supramolecular chemistry. Further research is needed to explore their full potential and to develop their practical applications.

Department of Chemistry, Faculty of Science, The University of Kufa, P. O. Box 21, Najaf 54001, Iraq. E-mail: ahmedh.alameri@uokufa.edu.iq

† Electronic supplementary information (ESI) available. CCDC 2247957–2247962. For ESI and crystallographic data in CIF or other electronic format see DOI: https://doi.org/10.1039/d3ra02913a

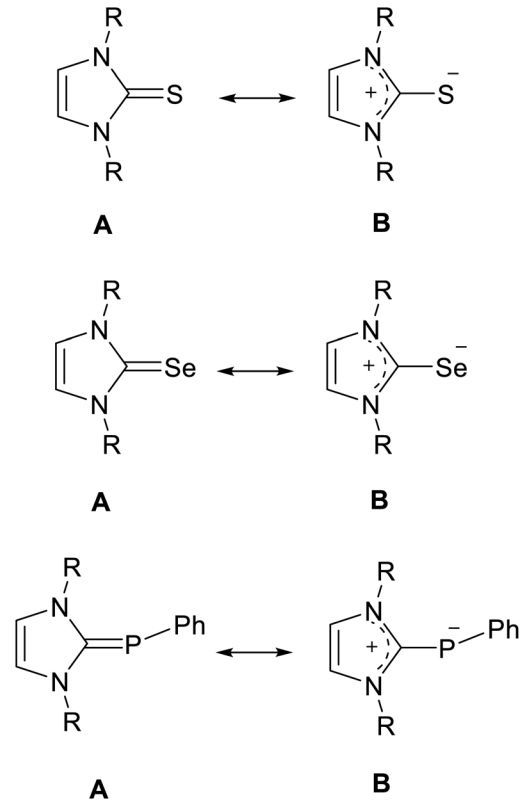

Fig. 1 Resonance structures of the NHC sulfur, selenium and phosphinidene adducts.

Results and discussion

Synthesis of the imidazole-2-selones

The cyclophanes incorporating imidazole-2-selone units **8–11** were synthesized by the reaction of the corresponding imidazolium-linked cyclophane salts with selenium and potassium carbonate in methanol at 60 °C overnight. The products were precipitated from the mixture and recrystallized to obtain a white powder with a moderate yield. The conformations of the cyclophanes incorporating imidazole-2-selone units **8–11** were characterized using X-ray diffraction and NMR methods.

Structures and conformations of imidazole-2-selones cyclophanes in solid state

Crystals **8**, **10** and **11** were grown by the slow evaporation of a solution of the relevant compound in CH_2Cl_2, while **9**·$(CHCl_3)_2$ was grown by the slow evaporation of a solution of the compound in $CHCl_3$. The results of crystallographic studies are summarized in Tables 1 and 2 and Fig. 3–8.

X-ray studies demonstrate that the conformation of cyclophanes incorporating imidazole-2-selone units **8–11** is broadly similar to that observed in the cyclophanes incorporating imidazole-2-thione units **4–7**. For *o*-cyclophane **8**, the benzene and imidazole-2-selone rings making a 'cup shape' and the orientation of C=Se groups are *exo* for the macrocyclic ring to yield conformation similar to the cone conformation of calix[4] arenes. The imidazole-2-selone rings are nearly parallel; therefore, the cup is slightly flattened. Obviously, the bending of the C=Se bonds out of the N_2C_2 planes of the imidazole-2-selones is a result of steric repulsion between the Se atoms (Fig. 3).

The molecule structures form pairs to obtain interlocking cup conformation. Then, the pairs accumulate into columns because of interactions between the benzene rings (intermolecular distance between C_6 planes is ~3.343 Å and 3.429 Å) (Fig. 4).

Mesitylene *m*-cyclophane **10** also has a conformation similar to the cone conformation of calix[4]arenes. However, in this case, the imidazole-2-selone rings are separated. Therefore, the unfavorable steric interactions between the Se atoms and the methyl substituents in each of the benzene rings are nonexistent, and the "cup conformation" is now completely pinched. Obviously, the structure of the *m*-cyclophane allows for the separation of the selone rings such that the C=Se bond is not bent outside the C_3N_2 plane (*cf.* the case of *o*-cyclophane **8**). The

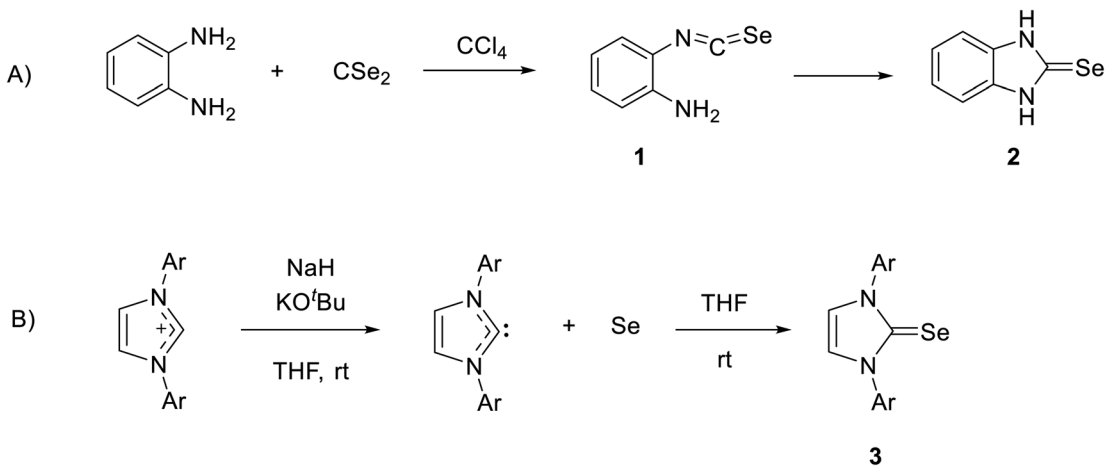

Scheme 1 (A) The first synthesis of selone by reaction of *o*-phenylenediamine with carbon diselenide. (B) Synthesis of stable selone by reaction of an imidazolium salt with Se.

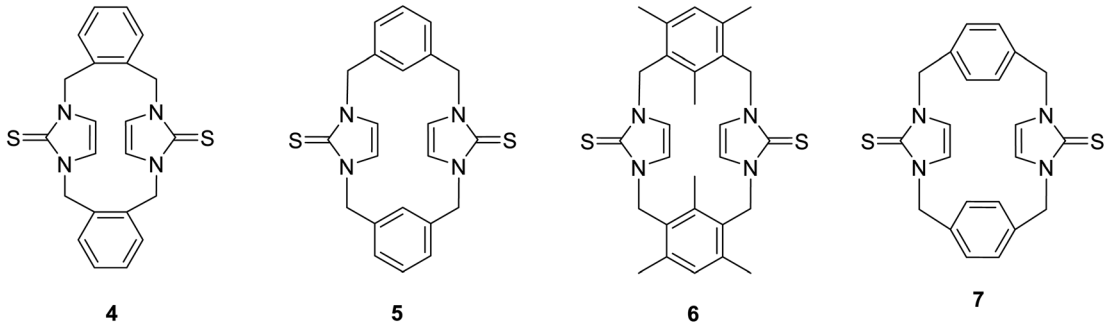

Fig. 2 Cyclophanes incorporating imidazole-2-thione moieties.

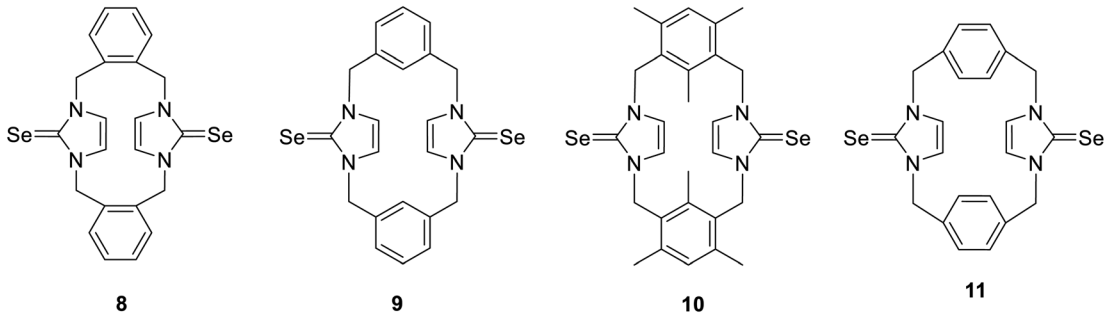

Table 1 Crystal data of **8**, **9**, **10** and **11**

Complex	**8**	**9**·$(CHCl_3)_2$	**10**	**11**	**11′**	**11″**
Empirical formula	$C_{22}H_{20}N_4Se_2$	$C_{24}H_{22}Cl_6N_4Se_2$	$C_{28}H_{32}N_4Se_2$	$C_{22}H_{20}N_4Se_2$	$C_{22}H_{20}N_4Se_2$	$C_{22}H_{20}N_4Se_2$
Formula weight	498.34	737.07	582.49	498.34	498.34	498.34
Wavelength/Å	1.54178	0.71073	1.54178	1.54178	1.54178	0.71073
Crystal system	Monoclinic	Monoclinic	Orthorhombic	Orthorhombic	Monoclinic	Monoclinic
Space group	$P2_1/n$	$P2_1/c$	*Pbcm*	*Pnma*	$P2_1/c$	$P2_1/c$
a/Å	17.8415 (4)	7.2960 (2)	11.533 (2)	12.3930 (8)	7.1187 (2)	9.1890 (4)
b/Å	10.5984 (3)	19.9813 (5)	12.4756 (13)	18.8028 (13)	14.2693 (6)	12.1051 (4)
c/Å	20.8127 (5)	9.9038 (2)	17.2625 (14)	8.6492 (4)	19.7393 (8)	9.9941 (4)
β/°	100.348 (2)	103.675 (2)	—	—	98.384 (4)	114.539 (5)
V/Å^3	3871.49 (17)	1402.88 (6)	2483.9 (5)	2015.5 (2)	1983.67 (13)	1011.27 (8)
Z	8	2	4	4	4	2
ρ(calc)/Mg m^{-3}	1.710	1.745	1.558	1.642	1.669	1.637
μ/mm^{-1}	4.894	3.230	3.902	4.700	4.776	3.671
Crystal size/mm^3	0.09 × 0.06 × 0.01	0.17 × 0.07 × 0.04	0.170 × 0.060 × 0.010	0.275 × 0.040 × 0.024	0.315 × 0.030 × 0.020	0.200 × 0.136 × 0.034
θ range for data collection/°	4.3 to 66.8	2.3 to 30.4	3.8 to 67.4	5.6 to 67.1	3.8 to 66.7	2.5 to 30.9
Reflections collected	19 568	29 526	11 654	17 634	17 396	10 805
Independent reflections	6875	4884	2302	1856	3530	3329
R(int)	0.0717	0.060	0.1747	0.1109	0.1204	0.0555
Max./min. transmission	1.00/0.918	1.00/0.923	1.00/0.658	1.00/0.695	1.00/0.875	1.00/0.756
Restraints/parameters	0/505	0/163	0/166	0/127	0/253	0/127
Goodness-of-fit on F^2	1.001	1.000	1.001	1.003	1.000	1.000
$R_1[I > 2\sigma(I)]$	0.0487	0.0383	0.0738	0.0721	0.0588	0.0469
w$R_2[I > 2\sigma(I)]$	0.1011	0.0838	0.1780	0.1832	0.1342	0.1053
R_1 (all data)	0.049	0.038	0.074	0.072	0.059	0.047
wR_2 (all data)	0.123	0.094	0.241	0.216	0.165	0.126
$\Delta\rho$(max/min)/e Å^{-3}	1.51/−0.51	0.56/−0.48	1.02/−1.01	1.50/−0.46	1.17/−0.66	0.95/−1.25
CCDC number	2247962	2247957	2247960	2247959	2247961	2247958

Table 2 Bond lengths (Å) and angles (°) in imidazole-2-selones

Compound	Se–C	N–C	N–C–Se
8	1.850 (6), 1.827 (6) 1.843 (6), 1.847 (6)	1.475 (7), 1.480 (7)	126.4 (4), 127.3 (4) 127.8 (4), 127.2 (4)
9	1.841 (2)	1.357 (3), 1.359 (3)	126.98 (16), 127.39 (17)
10	1.861 (10)	1.382 (13), 1.344 (14)	124.8 (9), 127.7 (7)
11	1.867 (8)	1.337 (10), 1.353 (9)	126.3 (6), 125.6 (6)
11′	1.849 (3)	1.359 (4), 1.366 (4)	126.8 (2), 127.8 (2)
11″	1.855 (7), 1.842 (7)	1.353 (9), 1.362 (9) 1.380 (9), 1.380 (9)	126.8 (5), 127.6 (5) 127.8 (5), 125.7 (5)

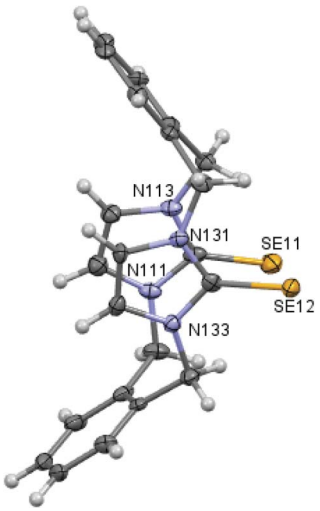

Fig. 3 Crystal structure (50% probability level for the displacement ellipsoids) of a single molecule of **8**. Selected bond lengths (Å) and angles (°): Se11–C112 1.850 (6), Se12–C132 1.827 (6), C11–N111 1.475 (7), C11–C142 1.520 (9), N111–C112–Se11 126.4 (4), N113–C112–Se11 127.3 (4), N131–C132–Se12 127.8 (4), N133–C132–Se12 127.2 (4).

observed conformation of **10** is similar to the conformation of the corresponding imidazole-2-thione **6** and contradicts the conformation of the parent imidazolium-linked cyclophane, in which the C2–H in the imidazolium moieties is oriented into the cavity formed between the mesitylene rings. The corresponding orientation of the imidazole thione or selone groups in **6** or **10** might be unfavorable because of the electron repulsion between the electron-rich C=S/Se groups.

In contrast to **8** and **10**, *m*-cyclophane **9** has an *anti* conformation (Fig. 6), which is similar to the 1,2-alternate conformation of calix[4]arene. The imidazole-2-selone rings are parallel, with their C=Se groups located in opposite directions *c*.

X-ray diffraction shows three crystal structures of *p*-cyclophane. First, in the crystal structure of *p*-cyclophane **11**, the C=Se groups in the imidazole-2-selone rings are oriented in the same direction to obtain a *syn* conformation (Fig. 7). The macrocycle of *p*-cyclophane **11** is in the form of approximately parallelepiped. The two imidazole-2-selone rings are almost parallel (dihedral angle 1.68°) and occupy opposite faces separated by a distance of about 6.517 Å, and the aryl groups are approximately parallel (dihedral angle 8.55°) and occupy two

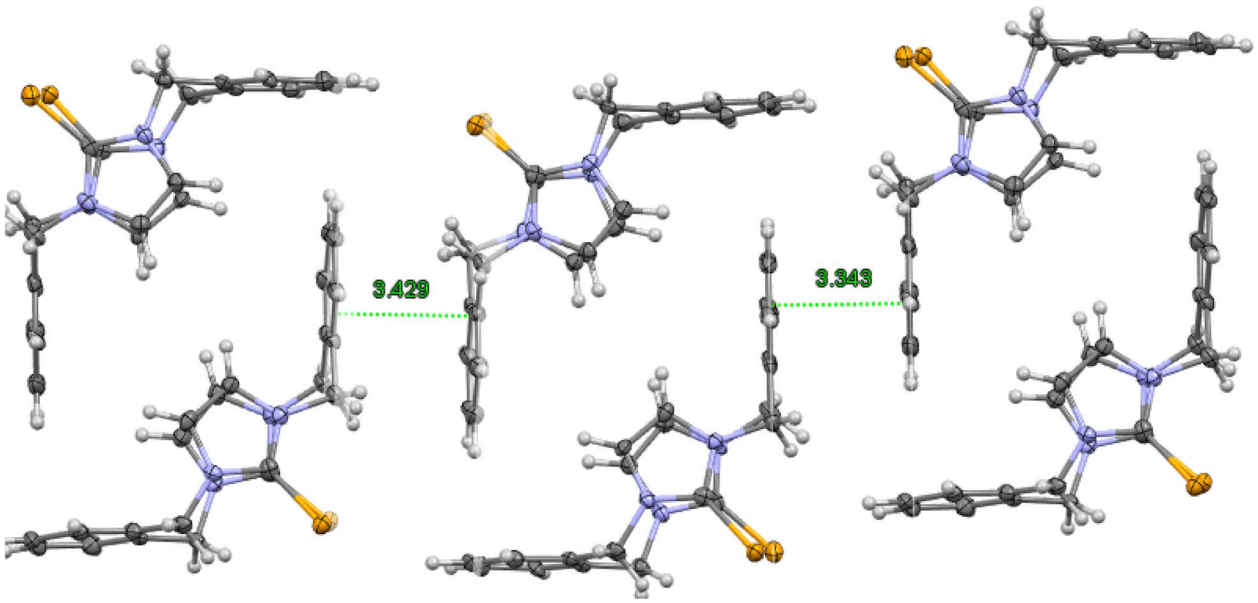

Fig. 4 Crystal structure (50% probability level for the displacement ellipsoids) of a column of interlocked pairs of **8**.

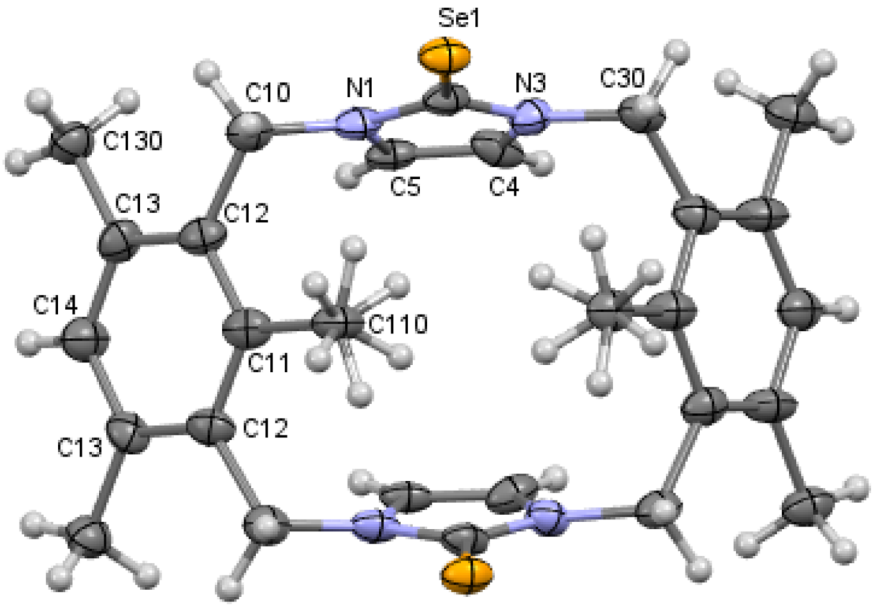

Fig. 5 Crystal structure (30% probability level for the displacement ellipsoids) of a single molecule of **10**. Selected bond lengths (Å) and angles (°): Se1–C2 1.861 (10), N1–C2 1.382 (13), C2–N3 1.344 (14), C4–C5 1.340 (15), N3–C2–Se1 127.7 (7), and N1–C2–Se1 124.8 (9).

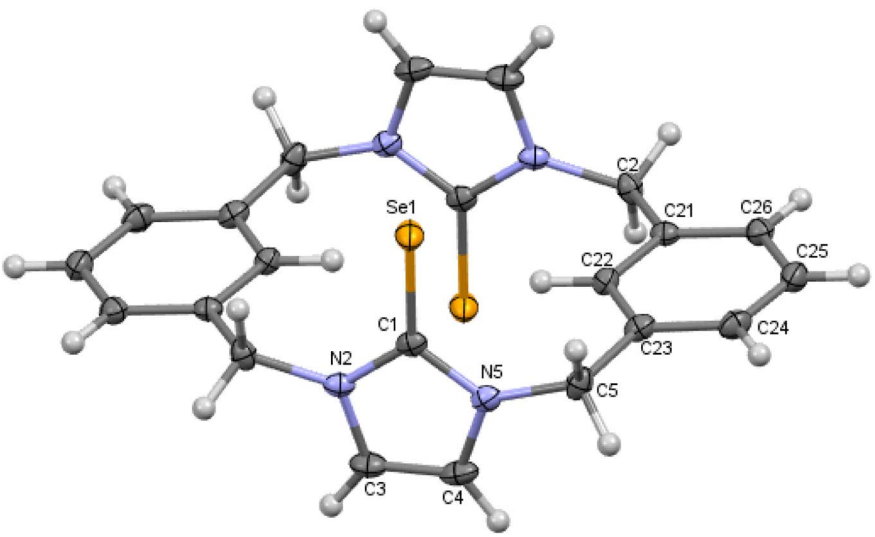

Fig. 6 Crystal structure (50% probability level for the displacement ellipsoids) of a single molecule of **9**. Selected bond lengths (Å) and angles (°): Se1–C1 1.841 (2), N2–C1 1.357 (3), C1–N5 1.359 (3), C4–C5 1.334 (3), N2–C1–Se1 126.98 (16), N5–C1–Se1 127.39 (17).

opposite faces separated by a distance of about 5.198 Å. The dihedral angles between the imidazole-2-selone and aryl group planes within the macrocycle are 89.84° and 89.72°. Obviously, there is some strain within the macrocycle. The bond between carbon methylene and carbon arene ring slightly deviates from the plane of the aryl group by 7.6 (4)°, and the bond between carbon methylene and nitrogen atom in the selone ring deviates from the plane of the imidazole-2-selone moiety by 12.3 (6)°.

Second, in the crystal structures of *p*-cyclophane (**11′** and **11″**), the C=Se groups in the imidazole-2-selone rings are oriented in opposite directions to obtain an *anti* conformation (Fig. 8). The macrocycle of *p*-cyclophane **11′** is also in the form of a parallelepiped (Fig. 8a). The two imidazole-2-selone rings are parallel (dihedral angle 0°) and occupy opposite faces separated by 6.283 Å; the aryl groups are also parallel (dihedral angle 0°), and the distance between the two opposite faces is about 5.464 Å. The dihedral angles between the imidazole-2-selone and aryl group planes within the macrocycle are 89.71 (10)°. As observed in **11**, there is also some strain within the macrocycle in **11′**. The bond between carbon methylene and carbon arene ring slightly deviates from the plane of the aryl group by 6.4 (3)°, and the bond between carbon methylene and nitrogen atom in the selone ring deviates from the plane of the imidazole-2-selone moiety by 10.9 (3)°. In contrast to **11** and **11′**, the macrocycle

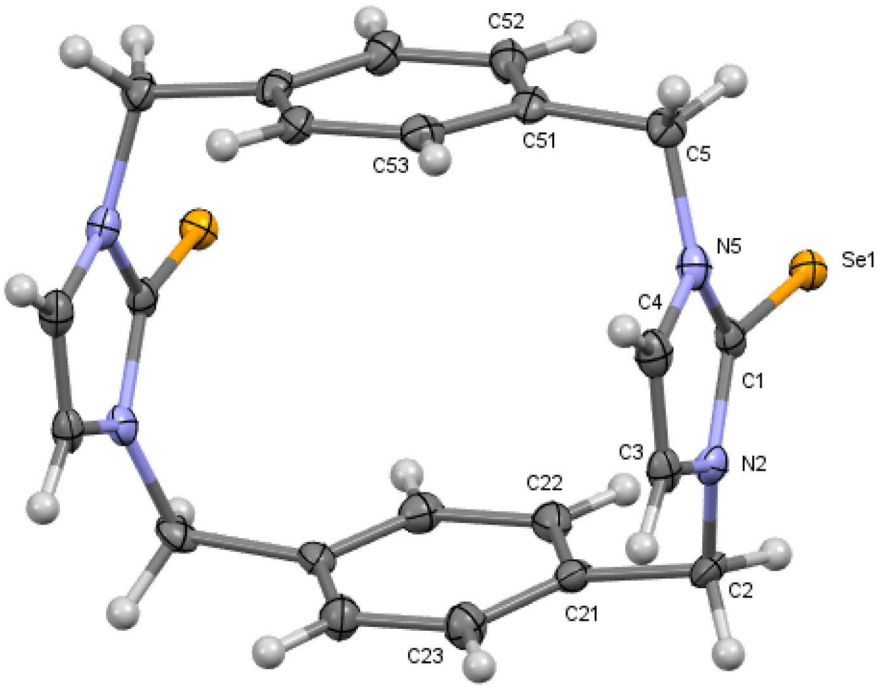

Fig. 7 Crystal structure (30% probability level for the displacement ellipsoids) of a single molecule of **11**. Selected bond lengths (Å) and angles (°): Se1–C1 1.867 (8), N2–C1 1.337 (10), C1–N5 1.353 (9), C4–C3 1.282 (11), N2–C1–Se1 126.3 (6), N5–C1–Se1 125.6 (6).

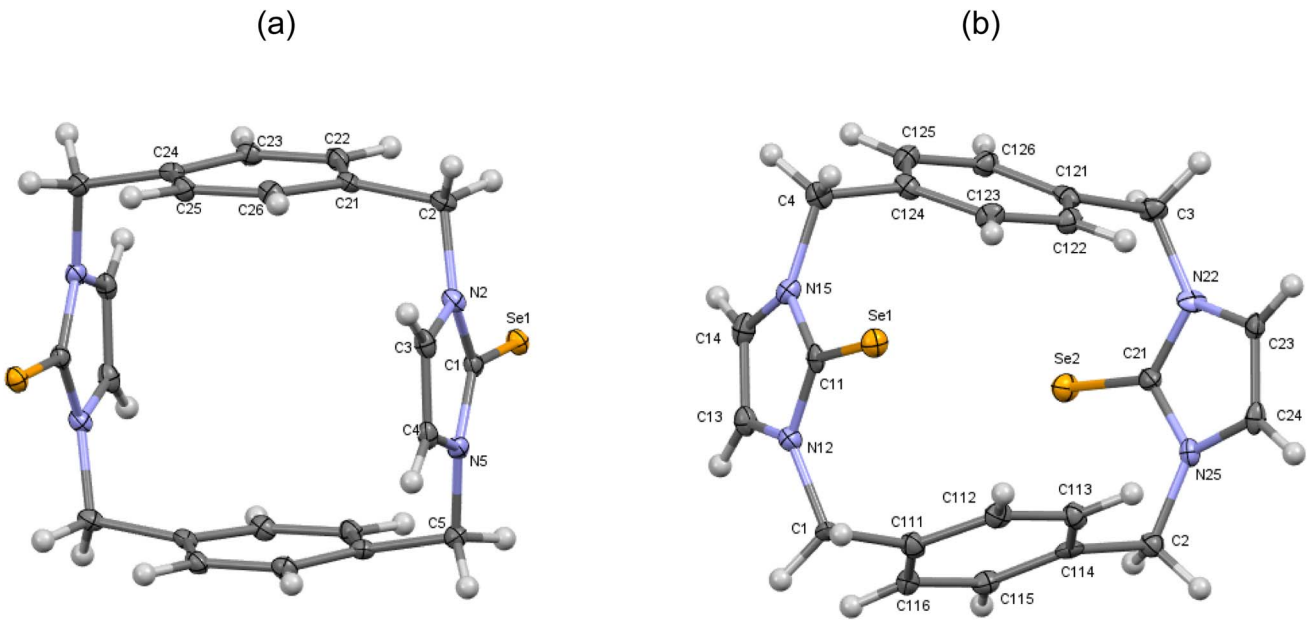

Fig. 8 (a) Crystal structure (30% probability level for the displacement ellipsoids) of a single molecule of **11′**. Selected bond lengths (Å) and angles (°): Se1–C1 1.849 (3), N2–C1 1.359 (4), C1–N5 1.366 (4), C4–C3 1.347 (5), N2–C1–Se1 126.8 (2), N5–C1–Se1 127.8 (2). (b) Crystal structure (30% probability level for the displacement ellipsoids) of a single molecule of **11″**. Selected bond lengths (Å) and angles (°): Se1–C11 1.855 (7), Se2–C21 1.842 (7), N15–C11 1.353 (9), C11–N12 1.362 (9), C14–C13 1.338 (11), N22–C21 1.380 (9), C21–N25 1.380 (9), C24–C23 1.331 (11), N15–C11–Se1 126.8 (5), N12–C11–Se1 127.6 (5), N22–C21–Se2 127.8 (5), N25–C21–Se2 125.7 (5).

of *p*-cyclophane **11″** adopts a conformation similar to the partial cone conformation of calix[4]arenes (Fig. 8b). The imidazole-2-selone rings are approximately parallel (dihedral angle 15.76°), and the C=Se bond in one of the selone rings is directed slightly into the cavity formed between the arene rings. Evidently, the aryl groups are now unparallel (dihedral angle 44.32°).

Table 3 ^{1}H NMR data[a] for imidazole-2-selones

Compound	CH_3	CH_2	H4/H5	Aromatics
8	—	4.65 (4H, d, $^2J_{H,H}$ 15 Hz) 5.80 (4H, d, $^2J_{H,H}$ 15 Hz)	5.88 (4H, s)	7.67–7.65, 7.54–7.52 (8H, AX pattern)
9[b]	—	5.73 (4H, d, $^2J_{H,H}$ 15 Hz) 4.96 (4H, d, $^2J_{H,H}$ 15 Hz) *5.89 (4H, d, $^2J_{H,H}$ 15 Hz)* *5.02 (4H, d, $^2J_{H,H}$ 15 Hz)*	7.31 (4H, s) *7.11 (4H, s)*	**7.43–7.39 (4H, m)** **7.35–7.31 (8H, m)** 6.25 (2H, s) *6.18 (2H, s)*
10	2.40 (12H, s) 1.55 (6H, s)	5.62 (4H, d, $^2J_{H,H}$ 15 Hz) 4.80 (4H, d, $^2J_{H,H}$ 15 Hz)	5.79 (4H, s)	7.01 (2H, s)
11[c]	—	5.54 (4H, d, $^2J_{H,H}$ 15 Hz) 4.66 (4H, d, $^2J_{H,H}$ 15 Hz) *5.22 (4H, d, $^2J_{H,H}$ 15 Hz)* *4.81 (4H, d, $^2J_{H,H}$ 15 Hz)*	7.42 (4H, s) *7.15 (4H, s)*	7.18 (8H, s) *7.48 (8H, s)*

[a] Recorded at 500.10 MHz and ambient temperature from solutions in DMSO-d_6. [b] Normal type indicates *anti* conformation, italics type indicates *syn* conformation, and bold type indicates overlapping signals of both conformations. [c] Normal type indicates *anti* conformation; italics type indicates *syn* conformation.

Conformation of imidazole-2-selone cyclophanes in a solution state

The NMR spectra of the imidazole-2-selone ligands in DMSO-d_6 solution at room temperature showed signals predicted for the suggested conformations (Table 3). The ^{1}H NMR spectrum of **8** is consistent with the structure shown in the solid state, in which the cyclophane macrocycle adopts a cone conformation. H4/H5 protons in the imidazole-2-selone ring show a remarkably upfield chemical shift (~5.88 ppm), which is an indication that the H4/H5 hydrogen atoms are shielded by the anisotropy of the cyclophane's benzene rings. Notably, the benzylic protons (*exo* and *endo* environments) show the pair of sharp doublets (~5.81 and ~4.65 ppm), which implies that the cone conformation of **8** is rigid on the NMR timescale. Obviously, the ^{1}H NMR spectrum of the **8** shows signals consistent with those seen in the corresponding imidazole-2-thione **4**,[18] while the ^{1}H NMR spectrum of the parent imidazolium cyclophane $\mathbf{12}^{2+}$ appears broad signals because the imidazolium cyclophane is rapidly interconverted to several conformations in solution[43] (Fig. 9). Presumably, the conformational ability of the imidazole-2-thione and imidazole-2-selone cyclophane structure decreased owing to an increase in bulkiness of the thione and selone groups in **4** and **8**, respectively, compared to the imidazolium groups in $\mathbf{12}^{2+}$.

The ^{1}H NMR spectrum (DMSO-d_6 solution at room temperature) of **10** is also consistent with the cone-type conformation in the solution, as observed in the solid state. Again, the ^{1}H NMR chemical shift of the H4/H5 protons in the imidazole-2-selone ring is markedly upfield chemical shift (~5.79 ppm, compared with ~8.02 ppm seen for H4/H5 protons in the parent imidazolium cyclophane $\mathbf{13}^{2+}$). Notably, the corresponding protons in imidazole-2-thione **6** are significantly upfield (~5.63 ppm). This upfield shift observed in **10** and **6** also indicates that the H4/H5 protons are shielded by the ring resonance of the benzene groups and, therefore, shows that the conformation in the solution is consistent with that seen in the solid state. H4/H5 protons in $\mathbf{13}^{2+}$ show a far downfield (8.02 ppm), and this indicates that the H4/H5 protons are deshielded by the effects of the benzene groups because of cyclophane formed in the 1,3-alternate type conformation and also due to the positive charge effects in the imidazolium rings. Interestingly, the pair of sharp doublets (*i.e.*, an AX pattern) for the benzylic protons (*exo* and *endo* environments) indicates that rapid interconversion between the two equivalent forms of this conformation does not occur in the solution. This provides additional evidence that the cone conformation is rigid in solution, as observed in the solid state. Rigidity of conformation has been shown similarly for the precursor imidazole-2-thione **6** and imidazolium-linked cyclophane $\mathbf{13}^{2+}$ (Fig. 10).[18,43]

The ^{1}H NMR spectrum of **9** shows two sets of signals with integrals in equal ratios (Fig. 11). These signals were assigned to two conformations based on different orientations of the two imidazole-2-selone moieties: one of them has *syn* conformation, and the other has *anti* conformation. In each conformation, the benzylic protons show one pair of doublets, indicating that both conformations of **9** are rigid on the NMR timescale (*i.e.* the rotation of imidazole-2-selone rings about their N–N axes do not occur in the solution). This result is consistent with the case for imidazole-2-thione **5** (ref. 18) and contradicts the parent imidazolium cyclophane $\mathbf{14}^{2+}$, which has conformational lability.[43] The two conformations are present in nearly equal amounts in the NMR timescale, and it is not able to assign the set signals in each conformation based on splitting patterns and chemical shifts. However, the crystals formed of **9** show only *anti* conformation based on the X-ray study (see above), while the powder formed of **9** presents as a *syn* conformation.

In both conformations of **9**, the splitting patterns and chemical shifts of the different proton environments are similar. Therefore, we are not able to assign a special conformation to a special set of signals in NMR. Notably, the similarity of signals in NMR shows that there is no interesting difference in shielding because of, for example, the resonance in arene rings. This interpretation is consistent with that seen in the solid state in which the arene rings are directed with their planes approximately parallel to the N–N axes of the imidazole-2-selone rings, so the environments of the CH_2 and H4/H5

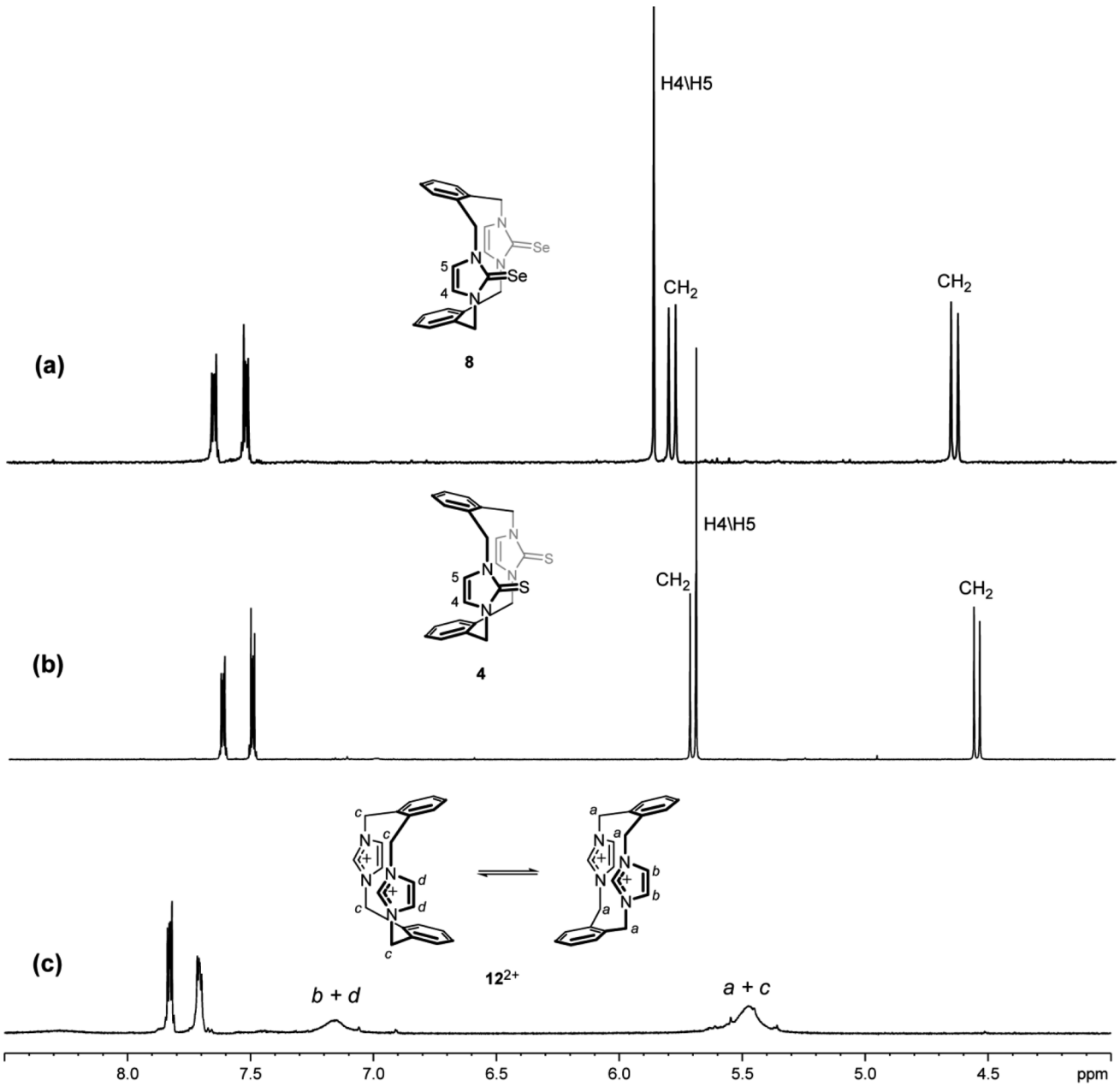

Fig. 9 Downfield region of the ^{1}H NMR spectra (500 MHz, DMSO-d_6) for solutions of (a) the ligand of imidazole-2-selone **8**, (b) the ligand of imidazole-2-thione **4** and (c) its precursor imidazolium-linked cyclophane salt **12**·2Br.

protons are away from the regions of shielding. These considerations apply to the *anti* and *syn* conformations.

The ^{1}H NMR spectra of **11** again show two sets of signals that are perhaps assigned to *syn* and *anti* conformations (Fig. 12). Obviously, both conformations are present in nearly equal amounts in the NMR timescale. Again, we are not able to assign the set signals to exact conformation based on chemical shifts and splitting patterns. Interestingly, the recrystallisation of **11** provided three types of crystals (as observed in the X-ray diffraction). The yellow needle crystals can be attributed to the *syn* conformation, and the colorless plate crystals can be attributed to the *anti* conformation based on the X-ray study, while the colorless needle crystals formed the other conformation attributed to the partial cone conformation. Notably, for *anti* and *syn* conformations of solutions of **11** in DMSO-d_6 and in acetone-d_6, arene ring protons H2′/H3′ should be shown as two environments. Therefore, in both cases, H2′/H3′ protons show one sharp single signal (even in acetone-d_6 at −25 °C). These considerations suggest that the arene rings are rapidly rotated about their C1′–C4′ axis on the NMR timescale (Fig. 13); therefore, a partial cone conformation does not appear in the solution, as seen in the solid state. The observed that two sets of NMR signals for *syn* and *anti* conformations indicate that the selone moieties are not rotated about their N–N axes on the NMR timescale.

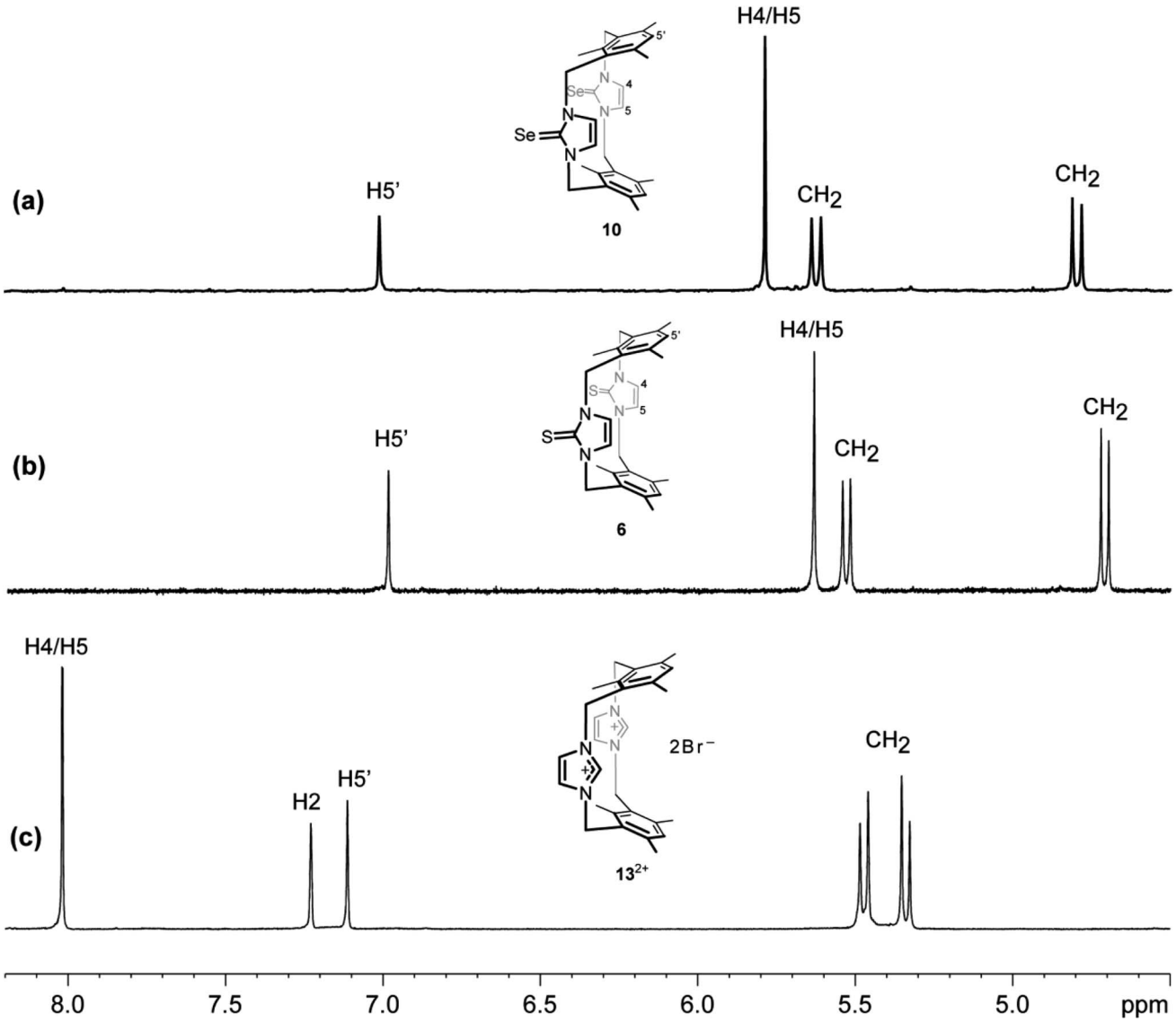

Fig. 10 Downfield region of the ^{1}H NMR spectra (500 MHz, DMSO-d_6) for solutions of (a) the ligand of imidazole-2-selone **10**, (b) the ligand of imidazole-2-thione **6** and (c) its precursor imidazolium-linked cyclophane salt **13**·2Br.

This result shows that both conformations are rigid in solution, as seen in the solid state. Obviously, the rigidity of conformation is similar to the precursor imidazole-2-thione **7** and imidazolium-linked cyclophane $\mathbf{15}^{2+}$ (Fig. 12).[18,43]

In the ^{13}C NMR spectra of the imidazole-2-selone ligands, the signal for the C=Se occurs in the range of 157 ppm, which is close to that reported for the related imidazole-2-selone,[13,34,44] but slightly upfield compared to that of the C=S (~163 ppm) in imidazole-2-thione ligands.[18]

DFT analysis

To investigate the relative stability of the different conformations of imidazole-2-selone cyclophanes, we conducted a series of calculations employing density functional theory (DFT) to interpret the origin of the stability of the crystal structures that we isolated experimentally. Four compounds were investigated with their possible spatial conformations **8** and **10** with three possible conformations: *syn*, where the two selone rings are oriented opposite to the xylylene rings; *anti*, where the C=Se group in selone rings is located on the opposite side of each other; and *syn_in*, where the two selone rings point toward the direction of the two aromatic rings. The other two conformations (**9** and **11**) have only two conformations (*syn* and *anti*) owing to their semi planar nature.

Fig. 14 shows the relative energies of the different conformations calculated using the Beck functional (BP86). The negative values indicate the energy preference of the *syn* geometries over the *anti* ones. From first glance, one can assume that pairs **8** and **10**, and **9** and **11** have the same energy trend in their conformational preferences. This assumption seems to be true for the latter geometries (**9** and **11**), where *anti* conformers tend to be marginally more stable over the *syn* structures in the semi planar molecules, which can explain the crystal co-existence of the two conformers. However, the above assumption is not true

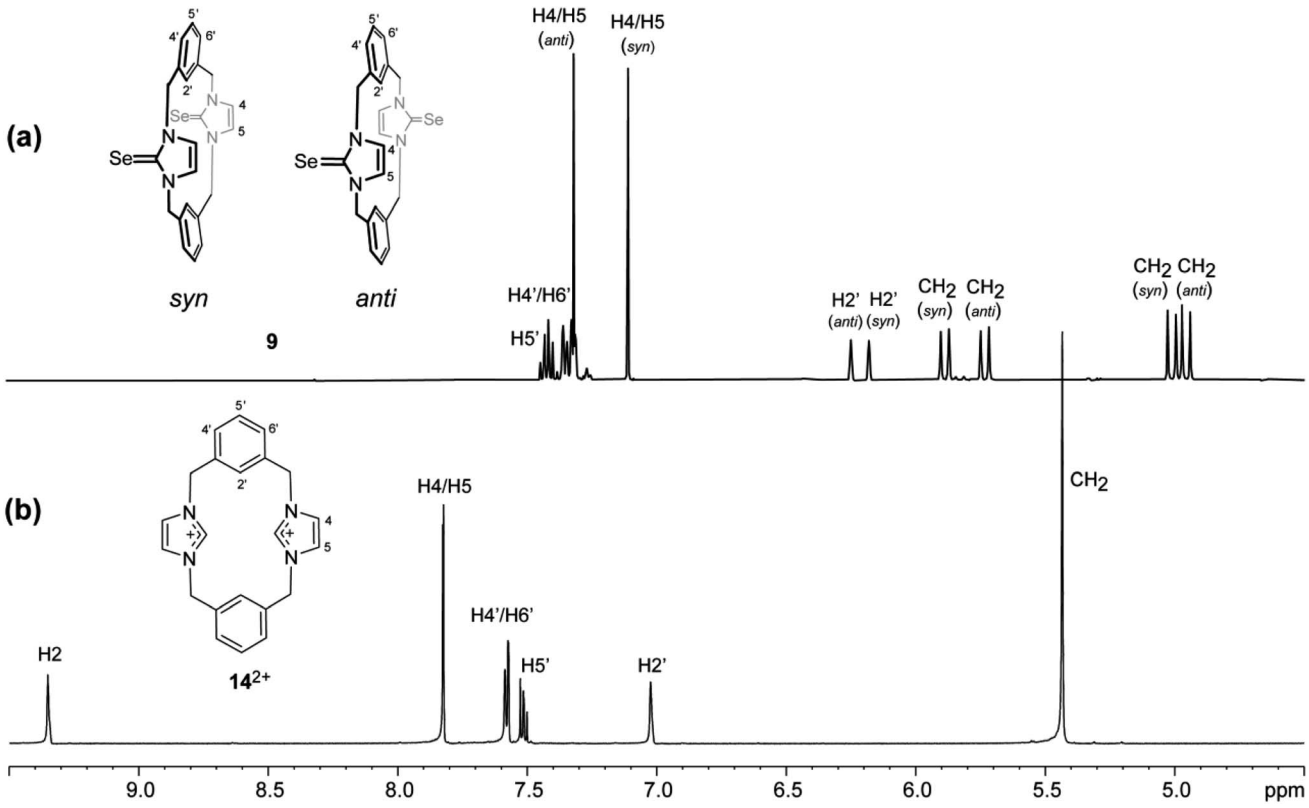

Fig. 11 Downfield region of the ^{1}H NMR spectra (500 MHz, DMSO-d_6) for solutions of (a) the ligand of imidazole-2-selone **9** and (b) its precursor imidazolium-linked cyclophane salt **14**·2Br.

for the **8** and **10** compounds. Although both the *anti* symmetric structures are not energetically preferred in these systems, the energy trends are contrasted when it comes to *syn_in* conformers. In **8** compounds, we see *syn* < *syn_in* < *anti* trend, and the **10** compound stability order is *syn* < *anti* < *syn_in*, where the *syn_in* is the least stable conformer. These computed figures agree with the experimental geometries for *syn* geometry that we isolated and reported in the experiments.

To shed light on the origin of the stability of the different conformers, we were inspired by Walsh's prominent orbital–structure correlation diagram.[45] For that, we illustrated the four of the highest occupied molecular orbitals (HOMOs) of both *syn* and *anti* conformers of **10** (Fig. 15). These energies contribute to a significant share influencing the final total energy of the system. The Kohn–Sham relative molecular orbitals were represented (eV) to facilitate the obvious contrast energy levels of the two conformers. The eigenvalues of the molecular states of the *syn* conformers recorded obvious stability over all the orbital energies of the *anti* conformers. The HOMO of the *anti c* destabilized the HOMO orbitals by 0.27 eV, while the HOMO-2 and HOMO-3 increase by only 0.10 eV and 0.11 eV, respectively. Similar justification can be drawn for the other conformational stabilities of the other of the structures shown in Fig. 14.

Conclusion

Imidazole-2-selone cyclophanes can be synthesized by reacting imidazolium cyclophanes with selenium in the presence of a mild base. These cyclophanes are stable white powdered compounds and were thoroughly characterized using X-ray diffraction, NMR spectroscopy, and mass spectrometry. Similar to the imidazole-2-thione cyclophanes, the imidazole-2-selone cyclophanes with selone groups connected by *o*-xylylene or mesitylene-*m*-xylylene rings exhibit only the *syn* conformation, while those with selone groups connected by *m*-xylylene or *p*-xylylene rings exhibit both *syn* and *anti* conformations. Unlike the parent imidazolium cyclophanes, which are conformationally labile, the synthesized thione and selone cyclophanes are significantly more conformationally rigid. Therefore, no interconversion between the *syn* and *anti* conformations can be detected on the NMR timescale. The geometrical analysis of various compounds was carried out by DFT calculation, and the calculations included the different possible conformations that resulted from orienting the selone groups in different directions. These calculations agree with the experimental data, which confirmed the stability of both *anti* and *syn* conformers in **9** and **11** compounds and the unique stability of *syn* geometries in **8** and **10**.

Experimental section

General procedures

Nuclear magnetic resonance spectra were recorded using a Bruker ARX500 (500.13 MHz for ^{1}H and 125.77 MHz for ^{13}C) or Bruker ARX 600 (600.13 MHz for ^{1}H, 150.90 MHz for ^{13}C) spectrometer at ambient temperature. ^{1}H and ^{13}C NMR chemical shifts were referenced to solvent resonance of the solvent

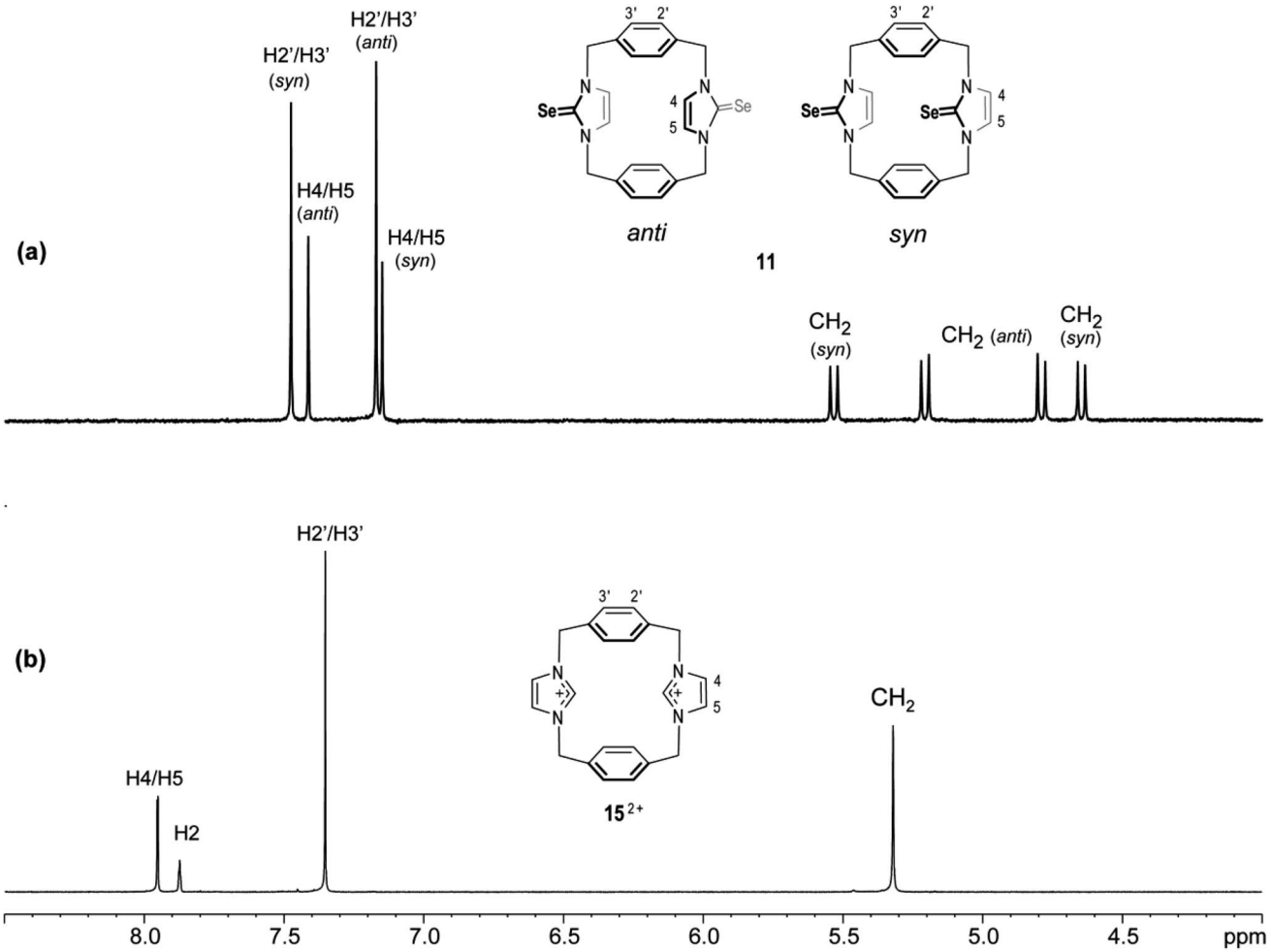

Fig. 12 Downfield region of the ^{1}H NMR spectra (500 MHz, DMSO-d_6) for solutions of (a) the ligand of imidazole-2-selone **11** and (b) its precursor imidazolium-linked cyclophane salt **15**·2Br.

(DMSO). When necessary, assignments were determined by ^{1}H–^{13}C HSQC (heteronuclear single quantum correlation) and ^{1}H–^{13}C HMBC (heteronuclear multiple bond coherence) spectra. Microanalyses were performed by The School of Chemistry and Molecular Bioscience, University of Queensland, Australia. High-resolution mass spectra were measured using Agilent LCMS 6510 Q-TOF and Waters LCT Premier XE spectrometers using the APCI method with MeCN : H_2O (9 : 1) as the solvent.

Synthesis of imidazole-2-selones

1. Synthesis of compound 8. A solution of *o*-cyclophane salt **12**·2Br (306 mg, 060 mmol) in CH_3OH (5 mL) was added to a mixture of selenium (99 mg, 1.25 mmol) and K_2CO_3 (165 mg, 1.25 mmol) in CH_3OH (15 mL). The mixture was refluxed for 48 h. The mixture was filtrated, and the solution was extracted with $CHCl_3$. The solvent was evaporated to obtain product **8** as a white powder (198 mg, 67%). Found: C, 51.92; H, 3.99; N, 10.92% $C_{22}H_{20}N_4Se_2(H_2O)_{0.5}$ requires C, 52.08; H, 4.17; N, 11.04%. ^{1}H NMR (500 MHz, DMSO-d_6): 7.67–7.65 (m, 4H, H4′/H5′), 7.54–7.52 (m, 4H, H3′/H6′), δ 5.88 (s, 4H, H4/H5), 5.81–5.79 (d, $^2J_{H,H}$ = 15 Hz, 4H, benzylic *H*CH), 4.67–4.64 (d, $^2J_{H,H}$ = 15 Hz, 4H, benzylic HC*H*). ^{13}C NMR (125.75 MHz, DMSO-d_6): δ 155.75 (C2), 134.94 (C1′/C2′), 133.72 (C3′/C6′), 129.63 (C4′/C5′), 118.49 (C4/C5), 50.91 (CH_2). HRMS (APCI$^+$): calcd for $C_{22}H_{20}N_4Se_2$ [M + H]$^+$, *m*/z 501.0097 found, *m*/z 501.0052.

2. Synthesis of compound 9. A solution of *m*-cyclophane salt **14**·2Br (209 mg, 0.40 mmol) in CH_3OH (5 mL) was added to a mixture of selenium (67 mg, 0.85 mmol) and K_2CO_3 (118 mg, 0.85 mmol) in CH_3OH (10 mL). The mixture was refluxed for 48 h. The mixture was filtrated, and the solution was extracted with $CHCl_3$. The solvent was evaporated to obtain product **9** as a white powder (120 mg, 60%). Found: C, 52.11; H, 3.97; N, 10.91% $C_{22}H_{20}N_4Se_2(H_2O)_{0.5}$ requires C, 52.08; H, 4.17; N, 11.04%. ^{1}H NMR (500 MHz, DMSO-d_6): *syn*; δ 7.43–7.39 (m, 4H, H5′), 7.35–7.31 (m, 8, H4′/H6′), 6.18 (s, 2H, H2′), 7.11 (s, 4H, H4/H5), 5.89 (d, $^2J_{H,H}$ = 15 Hz, 4H, benzylic *H*CH), 5.02 (d, $^2J_{H,H}$ = 15 Hz, 4H, benzylic *H*CH). *anti*; δ 7.43–7.39 (m, 4H, H5′), 7.35–7.31 (m, 8, H4′/H6′), 6.25 (s, 2H, H2′), 7.31 (s, 4H, H4/H5), 5.73 (d, $^2J_{H,H}$ = 15 Hz, 4H, benzylic *H*CH), 4.96 (d, $^2J_{H,H}$ = 15 Hz, 4H, benzylic *H*CH). ^{13}C NMR (125.75 MHz, DMSO-d_6): *syn*; δ 157.80 (C2), 137.52 (C1′/C3′), 128.48 (C5′), 126.20 (C4′/C6′), 122.12 (C2′),

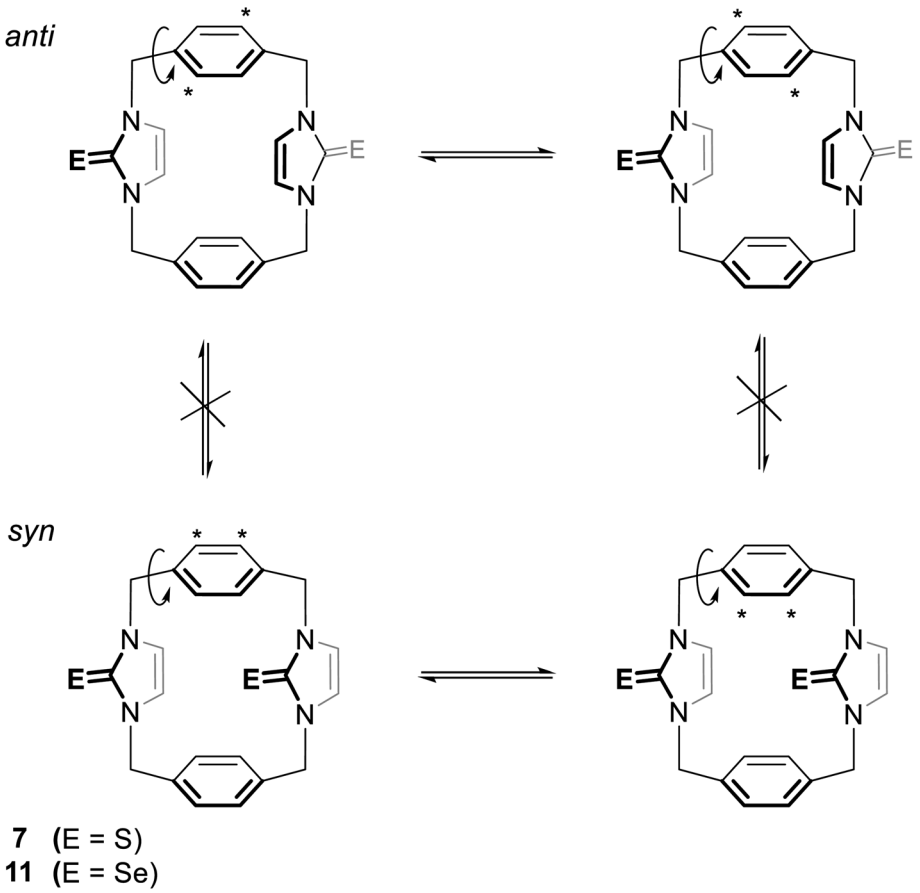

Fig. 13 The *syn* and *anti* conformations of **7** (ref. 18) and **11**. In each conformation, the asterisk refers to two equivalent protons on the arene rings. The rotation of this ring around its C1′–C4′ axis leads to the labeled protons replacing places with the unlabeled protons so that all the protons in the arene rings are equivalent.

120.42 (C4/C5), 51.29 (CH_2). *anti*; δ 156.95 (C2), 137.29 (C1′/C3′), 128.37 (C5′), 125.82 (C4′/C6′), 121.89 (C2′), 119.96 (C4/C5), 51.22 (CH_2). HRMS ($APCI^+$): calcd for $C_{22}H_{20}N_4Se_2$ $[M + H]^+$, *m*/z 501.0097 found, *m*/z 501.0067.

3. Synthesis of compound 10. A solution of mesityl-cyclophane salt **13**·2Br (235 mg, 0.40 mmol) in CH_3OH (5 mL) was added to a mixture of selenium (68 mg, 0.85 mmol) and K_2CO_3 (120 mg, 0.85 mmol) in CH_3OH (10 mL). The mixture was refluxed for 48 h. The mixture was filtrated, and the solution was extracted with $CHCl_3$. The solvent was evaporated to obtain product **10** as a white powder (134 mg, 58%). Found: C, 53.88; H, 5.23; N, 8.86% $C_{28}H_{32}N_4Se_2(CHCl_3)_{0.4}$ requires C, 54.12; H, 5.18; N, 8.89%. ^{1}H NMR (DMSO-d_6, 500 MHz): δ 7.01 (s, 2H, H5′), 5.79 (s, 4H, H4/H5), 5.64–5.61 (d, $^2J_{H,H}$ = 15 Hz, 4H, benzylic *H*CH), 4.81–4.78 (d, $^2J_{H,H}$ = 15 Hz, 4H, benzylic HC*H*), 2.40 (s, 12H, CH_3), 1.55 (s, 6H, CH_3). ^{13}C NMR (DMSO-d_6, 125.75 MHz): δ 156.45 (C2), 138.33 (C2′), 136.92 (C4′/C6′), 133.39 (C1′/C3′), 129.86 (C5′), 118.53 (C4/C5), 46.96 ($C_{benzylic}$), 19.57 (CH_3), 17.66 (CH_3). HRMS ($APCI^+$): calcd for $C_{28}H_{33}N_4Se_2$ $[M + H]^+$, *m*/z 585.1036. Found, *m*/z 585.1043.

4. Synthesis of compound 11. A solution of *p*-cyclophane salt **15**·2Br (152 mg, 0.30 mmol) in CH_3OH (5 mL) was added to a mixture of selenium (50 mg, 0.65 mmol) and K_2CO_3 (90 mg, 0.65 mmol) in CH_3OH (10 mL). The mixture was refluxed for 48 h. The mixture was filtrated, and the solution was extracted with $CHCl_3$. The solvent was evaporated to obtain product **11** as a white powder (105 mg, 52%). Found: C, 52.32; H, 3.93; N, 10.79% $C_{22}H_{20}N_4Se_2(H_2O)_{0.5}$ requires C, 52.08; H, 4.17; N, 11.04%. ^{1}H NMR (500 MHz, DMSO-d_6): *syn*; δ 7.48 (s, 8H, H2′/H3′), 7.15 (s, 4H, H4/H5), 5.23–5.20 (d, $^2J_{H,H}$ = 15 Hz, 4H, benzylic *H*CH), 4.82–4.79 (d, $^2J_{H,H}$ = 13 Hz, 4H, benzylic HC*H*). *anti*; δ 7.18 (s, 8H, H2′/H3′), 7.42 (s, 4H, H4/H5), 5.56–5.53 (d, $^2J_{H,H}$ = 15 Hz, 4H, benzylic *H*CH), 4.68–4.65 (d, $^2J_{H,H}$ = 15 Hz, 4H, benzylic HC*H*). ^{1}H NMR (500 MHz, acetone-d_6): *syn*; δ 7.66 (s, 8H, H2′/H3′), 6.99 (s, 4H, H4/H5), 5.88–5.85 (d, $^2J_{H,H}$ = 15 Hz, 4H, benzylic *H*CH), 4.64–4.61 (d, $^2J_{H,H}$ = 15 Hz, 4H, benzylic HC*H*). *anti*; δ 7.28 (s, 8H, H2′/H3′), 7.29 (s, 4H, H4/H5), 5.47–5.44 (d, $^2J_{H,H}$ = 15 Hz, 4H, benzylic *H*CH), 4.84–4.81 (d, $^2J_{H,H}$ = 15 Hz, 4H, benzylic HC*H*). HRMS ($APCI^+$): calcd for $C_{22}H_{20}N_4Se_2$ $[M + H]^+$, *m*/z 501.0097 found, *m*/z 501.0089.

Computational details

In this study, Kohn–Sham DFT was utilized to calculate the compounds under investigation. To optimize the geometry of the compounds, we utilized the general gradient

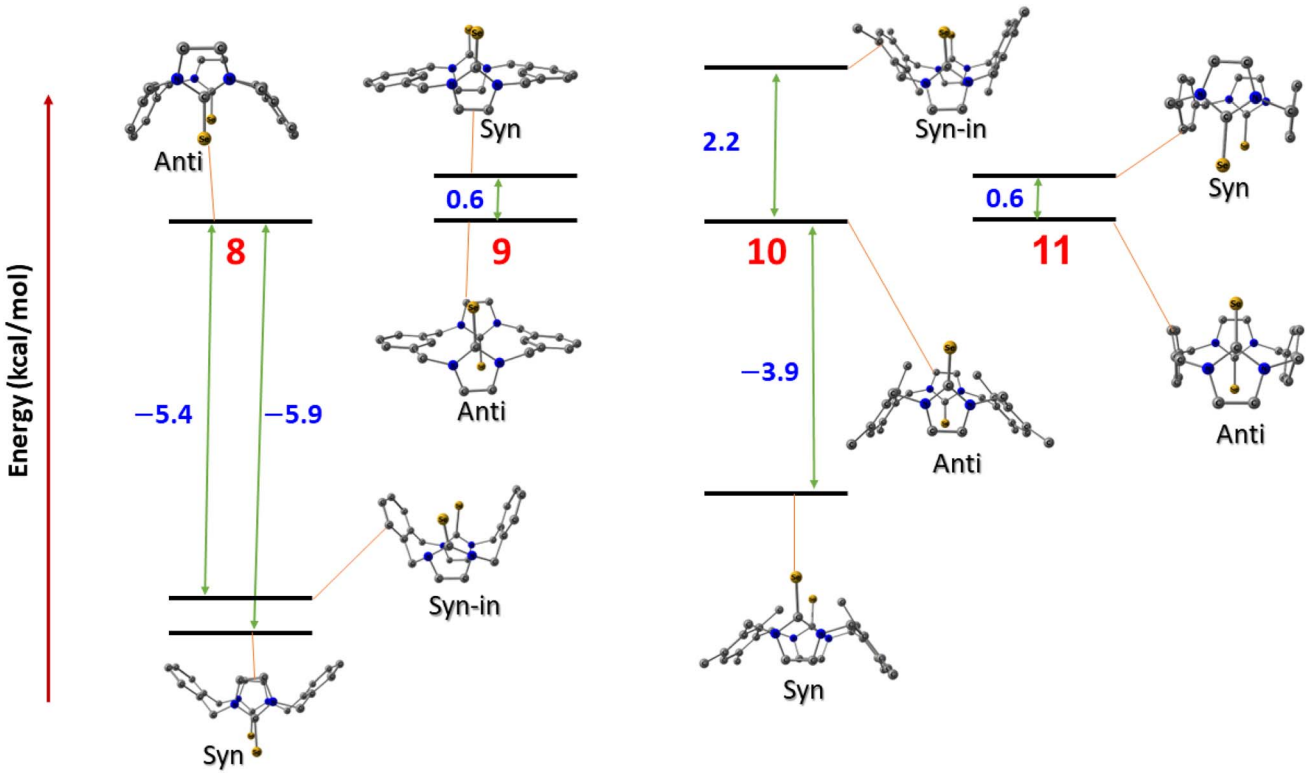

Fig. 14 The conformation relative energies in kcal mol^{-1} for imidazole-2-selones.

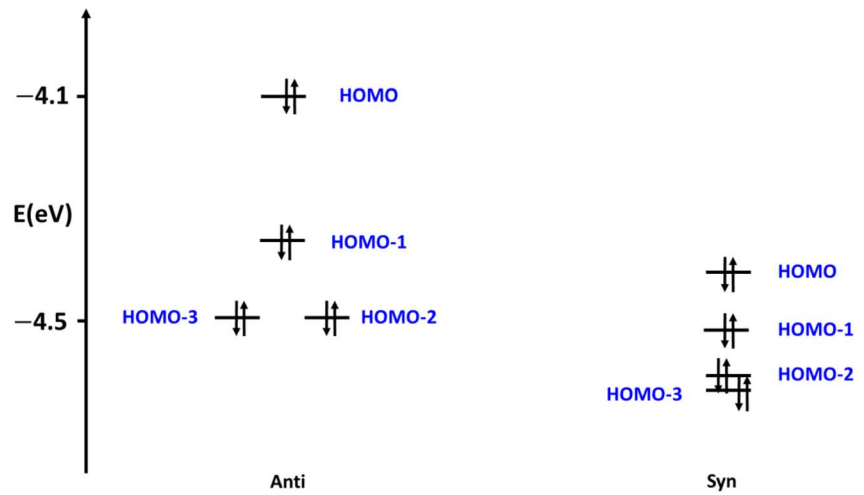

Fig. 15 The occupied frontier orbitals of **10** conformers.

approximation (GGA) functional BP86,[46,47] which was composed of the Becke 1988 exchange functional and the Perdew 86 correlation functional. For more accurate energies on the optimized geometries, Ahlrichs' triple zeta valence polarized (def2-TZVP)[48] basis set was employed, as well as the resolution of the identity (RI) approach and corresponding auxiliary basis sets,[49] along with Grimme's D3 dispersion correction.[50] All calculations were carried out using the Turbomole 7.3 package.

X-ray crystal structure determination

Crystals **8**, **10** and **11** were grown by the slow evaporation of a solution of the relevant compound in CH_2Cl_2, and crystals of **9**·$(CHCl_3)_2$ were grown by the slow evaporation of a solution of the compound in $CHCl_3$. Crystallographic data were collected at 100(2) K using either an Oxford Diffraction Gemini or an Oxford Diffraction Xcalibur diffractometer with Mo Kα or Cu Kα radiation. Following multi-scan or analytical absorption corrections and solution by direct methods, the structures were refined

against F^2 with full-matrix least-squares using the program SHELXL-2015.[51] Water molecule hydrogen atoms were refined with geometries restrained to ideal values. All remaining hydrogen atoms were added at calculated positions and refined using riding models with isotropic displacement parameters based on those of the parent atoms. Anisotropic displacement parameters were employed throughout the non-hydrogen atoms.

Author contributions

Ahmed Hassoon Mageed: conceptualization, investigation, methodology, writing – original draft. Karrar Al-Ameed: software, writing – review & editing.

Conflicts of interest

There are no conflicts to declare.

Acknowledgements

The authors acknowledge the facilities, and the scientific and technical assistance of the Australian Microscopy & Microanalysis Research Facility at the Centre for Microscopy, Characterisation & Analysis, The University of Western Australia.

References

1 M. N. Hopkinson, C. Richter, M. Schedler and F. Glorius, *Nature*, 2014, **510**, 485–496.
2 S. Diez-Gonzalez, N. Marion and S. P. Nolan, *Chem. Rev.*, 2009, **109**, 3612–3676.
3 W. A. Herrmann, *Angew. Chem., Int. Ed.*, 2002, **41**, 1290–1309.
4 S. Bellemin-Laponnaz and S. Dagorne, *Chem. Rev.*, 2014, **114**, 8747–8774.
5 M. Melaimi, M. Soleilhavoup and G. Bertrand, *Angew. Chem., Int. Ed.*, 2010, **49**, 8810–8849.
6 H. Valdés, D. Canseco-González, J. M. Germán-Acacio and D. Morales-Morales, *J. Organomet. Chem.*, 2018, **867**, 51–54.
7 A. H. Mageed, *J. Organomet. Chem.*, 2019, **902**, 120965.
8 A. H. Mageed, B. W. Skelton, A. N. Sobolev and M. V. Baker, *Eur. J. Inorg. Chem.*, 2018, **2018**, 109–120.
9 K. Al-Ameed and A. H. Mageed, *Polyhedron*, 2021, **205**, 115323.
10 O. Back, M. Henry-Ellinger, C. D. Martin, D. Martin and G. Bertrand, *Angew. Chem., Int. Ed.*, 2013, **52**, 2939–2943.
11 R. R. Rodrigues, C. L. Dorsey, C. A. Arceneaux and T. W. Hudnall, *Chem. Commun.*, 2014, **50**, 162–164.
12 A. Liske, K. Verlinden, H. Buhl, K. Schaper and C. Ganter, *Organometallics*, 2013, **32**, 5269–5272.
13 V. Rani, H. B. Singh and R. J. Butcher, *Eur. J. Inorg. Chem.*, 2017, **2017**, 3720–3728.
14 D. Sathyanarayana, S. K. Raja and R. Shunmugam, *Spectrochim. Acta, Part A*, 1987, **43**, 501–506.
15 E. Raper, J. Creighton, R. Oughtred and I. Nowell, *Acta Crystallogr., Sect. B: Struct. Sci.*, 1983, **39**, 355–360.
16 S. Sauerbrey, P. K. Majhi, G. Schnakenburg, A. J. Arduengo III and R. Streubel, *Dalton Trans.*, 2012, **41**, 5368–5376.
17 K. B. Wiberg and Y. Wang, *Arkivoc*, 2011, **45**, 56.
18 A. H. Mageed, B. W. Skelton, A. N. Sobolev and M. V. Baker, *Tetrahedron*, 2018, **74**, 2956–2966.
19 A. H. Mageed and K. Al-Ameed, *New J. Chem.*, 2021, **45**(39), 18433–18442.
20 A. Decken, C. J. Carmalt, J. A. Clyburne and A. H. Cowley, *Inorg. Chem.*, 1997, **36**, 3741–3744.
21 G. Kjellin and J. S. Strom, *Acta Chem. Scand.*, 1969, **23**, 2888–2899.
22 W.-G. Jia, Y.-B. Huang, Y.-J. Lin and G.-X. Jin, *Dalton Trans.*, 2008, 5612–5620.
23 N. Ghavale, S. T. Manjare, H. B. Singh and R. J. Butcher, *Dalton Trans.*, 2015, **44**, 11893–11900.
24 C. N. Babu, K. Srinivas and G. Prabusankar, *Dalton Trans.*, 2016, **45**, 6456–6465.
25 H.-N. Zhang, W.-G. Jia, Q.-T. Xu and C.-C. Ji, *Inorg. Chim. Acta*, 2016, **450**, 315–320.
26 A. K. Sharma, H. Joshi, R. Bhaskar and A. K. Singh, *Dalton Trans.*, 2017, **46**, 2228–2237.
27 G. Roy, M. Nethaji and G. Mugesh, *J. Am. Chem. Soc.*, 2004, **126**, 2712–2713.
28 Y. Yamashita and M. Yamashita, *J. Biol. Chem.*, 2010, **285**, 18134–18138.
29 A. Kamal, M. A. Iqbal and H. N. Bhatti, *Rev. Inorg. Chem.*, 2018, **38**, 49–76.
30 K. N. Sharma, N. Satrawala, A. K. Srivastava, M. Ali and R. K. Joshi, *Org. Biomol. Chem.*, 2019, **17**, 8969–8976.
31 W. Cao, L. Wang and H. Xu, *Nano Today*, 2015, **10**, 717–736.
32 A. Kamal, M. Nazari, M. Yaseen, M. A. Iqbal, M. B. K. Ahamed, A. S. A. Majid and H. N. Bhatti, *Bioorg. Chem.*, 2019, **90**, 103042.
33 J. Warner, *J. Org. Chem.*, 1963, **28**, 1642–1644.
34 D. J. Nelson, A. Collado, S. Manzini, S. Meiries, A. M. Slawin, D. B. Cordes and S. P. Nolan, *Organometallics*, 2014, **33**, 2048–2058.
35 M. Yaqoob, S. Gul, N. F. Zubair, J. Iqbal and M. A. Iqbal, *J. Mol. Struct.*, 2020, **1204**, 127462.
36 N. Iqbal, M. Yaqoob, M. Javed, M. Abbasi, J. Iqbal and M. A. Iqbal, *Comput. Theor. Chem.*, 2021, **1197**, 113135.
37 R. Ashraf, M. A. Iqbal, H. N. Bhatti, M. R. S. A. Janjua and M. El-Naggar, *ChemistrySelect*, 2020, **5**, 10970–10981.
38 H. Buhl, K. Verlinden, C. Ganter, S. B. Novaković and G. A. Bogdanović, *Eur. J. Inorg. Chem.*, 2016, **2016**, 3389–3395.
39 K. Verlinden, H. Buhl, W. Frank and C. Ganter, *Eur. J. Inorg. Chem.*, 2015, **2015**, 2416–2425.
40 S. Yadav, R. Deka and H. B. Singh, *Chem. Lett.*, 2019, **48**, 65–79.
41 M. S. S. Jamil and N. A. Endot, *Molecules*, 2020, **25**, 5161.
42 S. V. Vummaleti, D. J. Nelson, A. Poater, A. Gómez-Suárez, D. B. Cordes, A. M. Slawin, S. P. Nolan and L. Cavallo, *Chem. Sci.*, 2015, **6**, 1895–1904.
43 M. V. Baker, M. J. Bosnich, D. H. Brown, L. T. Byrne, V. J. Hesler, B. W. Skelton, A. H. White and C. C. Williams, *J. Org. Chem.*, 2004, **69**, 7640–7652.

44 M. T. Aroz, M. C. Gimeno, M. Kulcsar, A. Laguna and V. Lippolis, *Group 11 Complexes with Imidazoline-2-thione or Selone Derivatives*, Wiley Online Library, 2011.
45 T. A. Walsh, *Adv. Chem. Phys.*, 1953, **2**, 171–290.
46 J. P. Perdew, *Phys. Rev. B: Condens. Matter Mater. Phys.*, 1986, **33**, 8822.
47 A. D. Becke, *Phys. Rev. A: At., Mol., Opt. Phys.*, 1988, **38**, 3098.
48 K. Eichkorn and O. Treutler, *Chem. Phys. Lett.*, 1995, **240**, 283.
49 F. Weigend, *Phys. Chem. Chem. Phys.*, 2002, **4**, 4285–4291.
50 S. Grimme, J. Antony, S. Ehrlich and H. Krieg, *J. Chem. Phys.*, 2010, **132**, 154104.
51 G. M. Sheldrick, *Acta Crystallogr., Sect. C: Struct. Chem.*, 2015, **71**, 3–8.